

International Conference on Martensitic Transformations, ICOMAT-2014

## Dynamic stabilization of cubic AuZn

L. Isaeva<sup>a,\*</sup>, O. Hellman<sup>b,c</sup>, J. C. Lashley<sup>d</sup>, I. A. Abrikosov<sup>b</sup>, O. Eriksson<sup>a</sup>

<sup>a</sup>Division of Materials Theory, Department of Physics and Astronomy, Uppsala University, PO Box 516, 751 20 Uppsala, Sweden

<sup>b</sup>Department of Physics, Chemistry and Biology (IFM), Linköping University, SE-581 83, Linköping, Sweden

<sup>c</sup>Department of Applied Physics and Materials Science, California Institute of Technology, Pasadena, California 91125, USA

<sup>d</sup>Materials Science and Technology Division, Los Alamos National Laboratory, P.O. Box 1663, Bikini Atoll Road, Los Alamos, NM 87545, USA

---

### Abstract

A recently developed temperature-dependent effective potential method is employed to study the martensitic phase transformation in AuZn. This method is based on *ab initio* molecular dynamics and allows to obtain finite-temperature lattice vibrational properties. We show that the transversal acoustic TA<sub>2</sub>[110] mode associated with the phase transition is stabilized at 300 K. Temperature evolution of single-phonon dynamic structure factor at the wave vector  $\mathbf{q}=1/3[1,1,0]$ , associated with phonon softening and Fermi surface nesting, was also studied.

© 2015 The Authors. Published by Elsevier Ltd. This is an open access article under the CC BY-NC-ND license (<http://creativecommons.org/licenses/by-nc-nd/4.0/>).

Selection and Peer-review under responsibility of the chairs of the International Conference on Martensitic Transformations 2014.

**Keywords:** Lattice dynamics; anharmonicity; shape-memory alloys

---

### 1. Introduction

The shape-memory effect in equiatomic AuZn is associated with reversible martensitic transition,  $T_M=64$  K [1], which is only accessible using cryogenics. In this phase transition a high-temperature cubic phase of the CsCl-type, referred further to as B2 phase, transforms into monoclinic a low-temperature phase of the LiSn-type [2]. An increase in the Au concentration in the AuZn compound lowers the phase transition temperature: from 90 K in Au<sub>0.47</sub>Zn<sub>0.53</sub> down to 40 K in Au<sub>0.52</sub>Zn<sub>0.48</sub> [3]. The structural transition in off-stoichiometric AuZn is proven to have a

---

\* Corresponding author. Tel.: +46-18-471-3102; fax: +46-18-471-3524.

E-mail address: [leyla.isaeva@physics.uu.se](mailto:leyla.isaeva@physics.uu.se)

first-order character, typical for displacive phase transitions. However, in case of equiatomic composition the order of this phase transition is a matter of debate [4,5]. The de Haas - van Alphen oscillations observed in the magnetic susceptibility of AuZn indicate Fermi surface coexistence down to 60 mK [6] therefore suggesting a first-order type behavior. At the same time, the measured temperature dependence of the Bragg peak intensity implies a continuous transition [5]. Theoretical methods including a phenomenological Landau-Ginzburg approach have been also used to study the order of the phase transition and it has been shown that the phase transition is of first [7] or weakly first order character [5].

A premartensitic region usually exhibits anomalies in the phonon dispersion relations. An anomaly in AuZn phonon spectra appears as a softening of the transversal acoustic mode  $TA_2$  along the [110] direction indicating lattice instability with respect to (110)[1 10] shear distortions. Due to thermal expansion of the lattice, phonon frequencies are expected to decrease with increasing temperature, however, in AuZn the  $TA_2$  mode exhibits opposite behavior [1]. Similar anomalies have been observed in off-stoichiometric AuZn [1,6], and in other Hume-Rothery alloys with 3:2 electron per atom concentration [8-11]. The  $TA_2$  mode in AuZn softens down to the transition temperature while not reaching zero frequency, precluding the use of the soft-mode theory for its description [7]. Previously, we have applied first-principle theory to study the mechanism of the structural phase transformation in AuZn [7]. We have examined the topology of the Fermi surface and found nesting at Fermi surface with the translational vector  $\mathbf{q}=1/3[1,1,0]$  which is associated with the soft  $TA_2$ [110] mode. Thus, we concluded that coupling between lattice vibrations and nesting at the Fermi surface is responsible for the phase transition in AuZn. Here we extend our previous study by including finite temperature consideration of the lattice dynamics of cubic AuZn. This is realized by the newly developed temperature-dependent effective potential method [12,13].

## 2. Method

First-principles calculations were performed using *ab initio* molecular dynamics and projector augmented wave (PAW) [14,15] method as it is implemented within Vienna *ab initio* simulations package (VASP) [16-18]. Exchange-correlation effects were treated in the framework of the local density approximation (LDA) with the Ceperly-Alder functional [19]. A supercell of the cubic B2 AuZn phase containing 250 atoms was considered, and it was generated by increasing lattice parameters 5 times along each of the lattice vectors. The effect of lattice expansion were not taken into account and the experimental lattice parameter of 3.13 Å [20] was used throughout the study. Born-Oppenheimer molecular dynamics was performed using canonical (NVT) ensembles. Nosé thermostat was used to control the temperature of the system [21]. The time step used in all calculations is 1 fs. The duration of the molecular dynamics was 14 ps to ensure the convergence of the interatomic forces. Integration over the Brillouin zone was performed using Gaussian band smearing and 2x2x2 k-point mesh generated according to Monkhorst-Pack scheme. The plane wave cutoff energy was set to 450 eV.

Finite temperature vibrational properties of AuZn were calculated using the recently developed temperature-dependent effective potential (TDEP) method [12,13]. The TDEP method allows to accurately describe finite temperature lattice dynamical properties of crystals by implicitly accounting for the anharmonic effects. This is realized by finding the best possible harmonic (or higher order) Hamiltonian that can be mapped to the temperature-dependent potential energy at given volume and temperature. In this method interatomic force-constant matrices are calculated by minimizing the difference between the Hellman-Feynman forces which are obtained from molecular dynamics trajectories and the corresponding forces from the harmonic model. More details on the TDEP method can be found elsewhere [12,13,22].

## 3. Results

Phonon dispersion relations of B2 AuZn calculated with TDEP method at  $T = 300$  K using third-order force constants are shown in the left hand side of Fig. 1. The third-order force constants were calculated employing a generalization of TDEP described in [22]. More intense and broadened phonon branches correspond to those with larger linewidths and, correspondingly, shorter lifetimes. The calculated spectrum has no anomalies, indicating that

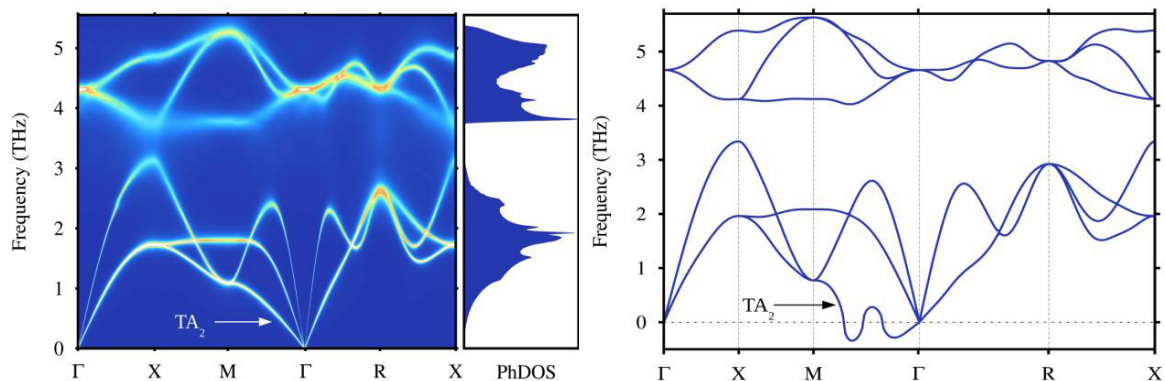


Fig. 1. Phonon dispersion relations and phonon density of states (PhDOS) calculated for B2 AuZn at 300 K using TDEP technique (left) and at 0 K using harmonic approximation (right).

B2 AuZn is dynamically stable at  $T = 300$  K. Inelastic x-ray scattering measurements show considerable phonon softening in the vicinity of the wave vector  $\mathbf{q}=1/3[1,1,0]$  which indicates an onset of the instability along the  $TA_2$  branch [1,5]. Conventional methods of calculating vibrational properties of materials, such as linear response [23] or small displacement methods [24], which allow only harmonic description of materials at 0 K, have been applied in our previous study [7]. There we obtained an imaginary acoustical  $TA_2$  branch along the  $\Gamma$ -M direction of the Brillouin zone with the dip in frequency near  $\mathbf{q}=1/3[1,1,0]$  (also shown here in the right panel of Fig. 1). However, in the present calculation no inflection in the transverse  $TA_2$  mode is found. We relate this to the smearing of the Fermi surface due to thermal atomic fluctuations from the ideal lattice positions. The phonon frequency of the transversal acoustic  $TA_2$  mode at the M(0.5,0.5,0) point is slightly overestimated in our calculations ( $\omega_M = 1.08$  THz) compared to the experimental value at  $T = 300$  K [5] ( $\omega_M = 0.89$  THz). The phonon density of states shows a gap between the optical and acoustic part of the spectrum which is about 0.58 THz.

The dynamic structure factor,  $S(\mathbf{q},\omega)$ , is a measure of the spatio-temporal particle (in our case, phonon) correlations in the material and is experimentally accessible by inelastic neutron-scattering measurements. Therefore, we have also calculated single-phonon dynamic structure factor for a few temperatures above the martensitic transition temperature ( $T = 100$  K, 200 K and 300 K) at the wave vector  $\mathbf{q}=1/3[1,1,0]$  using analytical expression in [25], and our results are presented in Fig.2. Note that Fig. 2 represents the same information shown in Fig. 1, but for a specific  $\mathbf{q}$  only. For calculation of the dynamic structure factor the third-order force constants were included [22]. Fig. 2 shows six peaks corresponding to the six phonon modes, with the lowest frequency peak (in light blue color) corresponding to the transverse acoustical  $TA_2$  branch. From Fig.2 it is clear that the widths of all the peaks broaden and shift towards larger frequencies as temperature increases. The one-phonon peak for the  $TA_2$  branch is centered at  $\omega \approx 0.77$  THz at  $T = 100$  K. This peak is shifted towards  $\omega \approx 0.81$  THz at  $T = 200$  K, and  $\omega \approx 0.92$  THz at  $T = 300$  K.

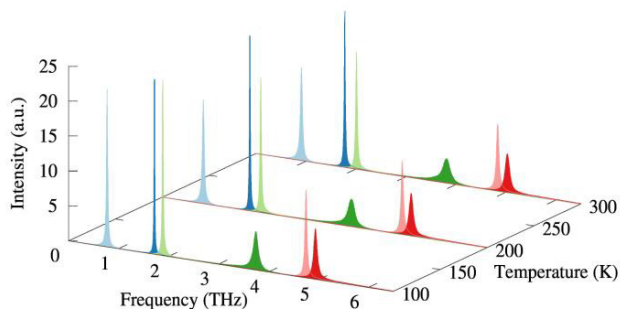


Fig. 2. Temperature dependent single-phonon dynamic structure factor calculated at  $\mathbf{q}=1/3[1,1,0]$  for B2 AuZn.

It is instructive to correlate the full width at half maximum (FWHM) of the structural factor  $S(\mathbf{q}, \omega)$  for TA<sub>2</sub> phonon branch at  $\mathbf{q}=1/3[1,1,0]$  with corresponding phonon lifetimes. Phonon lifetimes due to phonon-phonon scattering events can be calculated via  $\tau_{q,s} = 1/(2\Gamma_{q,s})$ , where  $\tau_{q,s}$  is lifetime of the phonon with wave vector  $\mathbf{q}$  and polarization  $s$ , and  $\Gamma_{q,s}$  is the imaginary part of the phonon self-energy. We obtain the following values for the imaginary part of the phonon self-energy:  $\Gamma_{q,s} \approx 0.013$  THz at  $T = 100$  K,  $\Gamma_{q,s} \approx 0.019$  THz at  $T = 200$  K, and  $\Gamma_{q,s} \approx 0.021$  THz at  $T = 300$  K. Therefore phonon lifetimes are  $\tau_{q,s} \approx 39$  ps at  $T = 100$  K,  $\tau_{q,s} \approx 27$  ps at  $T = 200$  K, and  $\tau_{q,s} \approx 23$  ps at  $T = 300$  K, respectively. As expected, phonon lifetimes become shorter at higher temperatures.

#### 4. Summary

In summary, the temperature-dependent effective potential method has been used to show thermal stabilization of B2 AuZn. Theoretical phonon dispersion relations show no peculiarities at 300 K, and the material is dynamically stable, in agreement with the experimental data. The absence of inflection in TA<sub>2</sub> mode along the  $\Gamma$ -M direction we associate to the smearing of the Fermi surface due to thermal atomic fluctuation introduced in molecular dynamics simulations. Calculated dynamical structure factor for the  $\mathbf{q}=1/3[1,1,0]$  shows broadening with the increase of temperature and shift towards larger energies.

#### Acknowledgements

We acknowledge the Swedish Research Council (VR), ERC (Grant No.247062), eSENCE, and KAW foundation for financial support. We also acknowledge Swedish National Infrastructure for Computing (SNIC) for the allocation in high performance supercomputers at NSC Linköping.

#### References

- [1] T. Makita, A. Nagasawa, Y. Morii, N. Minakawa, H. Ohno, Phys. B 213 (1995) 430.
- [2] M.H. Sahlberg, J.C. Lashley, Private communication.
- [3] R.D. McDonald, J. Singleton, P.A. Goddard, F. Drymiotis, N. Harrison, H. Harima, M.-T. Suzuki, A. Saxena, T. Darling, A. Migliori, J. L. Smith, J.C. Lashley, J. Phys.: Condens. Matter 17 (2005) L69.
- [4] M. Sanati, R.C. Albers, T. Lookman, A. Saxena, Phys. Rev. B 88 (2013) 024110.
- [5] J.C. Lashley, S. M. Shapiro, B. L. Winn, C. P. Opeil, M. E. Manley, A. Alatas, W. Ratcliff, T. Park, R. A. Fisher, B. Mihaila, P. Riseborough, E. K. H. Salje, J. L. Smith, Phys. Rev. Lett. 101 (2008) 135703.
- [6] P. A. Goddard, J. Singleton, R.D. McDonald, N. Harrison, J.C. Lashley, H. Harima, M.-T. Suzuki, Phys. Rev. Lett. 94 (2005) 116401.
- [7] L. Isaeva, P. Souvatzis, O. Eriksson, J.C. Lashley, Phys. Rev. B 89 (2014) 104101.
- [8] H. Tietze, M. Mullner, B. Renker, J. Phys. C 17 (1984) L529.
- [9] S.M. Shapiro, B.X. Yang, Y. Noda, L.E. Tanner, D. Schryvers, Phys. Rev. B 44 (1991) 9301.
- [10] E.I. Isaev, A.I. Lichtenstein, Yu.Kh. Vekilov, E.A. Smirnova, I.A. Abrikosov, S.I. Simak, R. Ahuja, B. Johansson, Solid State Commun. 129 (2004) 809.
- [11] T. Ohba, Phase Transitions 69 (1999) 289.
- [12] O. Hellman, I.A. Abrikosov, S.I. Simak, Phys. Rev. B 84 (2011) 180301.
- [13] O. Hellman, P. Steneteg, I.A. Abrikosov, S.I. Simak, Phys. Rev. B 87 (2013) 104111.
- [14] G. Kresse and D. Joubert, Phys. Rev. B 59 (1999) 1758.
- [15] P. E. Blöchl, Phys. Rev. B 50 (1994) 17953.
- [16] G. Kresse, J. Hafner, Phys. Rev. B 48 (1993) 13115.
- [17] G. Kresse, J. Furthmüller, Comput. Mater. Sci. 6 (1996) 15.
- [18] G. Kresse, J. Furthmüller, Phys. Rev. B 54 (1996) 11169.
- [19] D.M. Ceperley, B.J. Alder, Phys. Rev. Lett. 45 (1980) 566.
- [20] K. Krompholz, A. Weiss, Bes. Bunsenges. Phys. Chem. 82 (1978) 334.
- [21] S. Nosé, Progr. Theor. Phys. Suppl. 103 (1991) 1.
- [22] O. Hellman, I.A. Abrikosov, Phys. Rev. B 88 (2013) 144301.
- [23] S. Baroni, S. de Gironcoli, A. Dal Corso, P. Giannozzi, Rev. Mod. Phys. 73 (2011) 515.
- [24] D. Alfe, Comput. Phys. Commun. 180 (2009) 2622.
- [25] R.A. Cowley, Rep. Prog. Phys. 31 (1968) 123.